Future Deeply Inelastic Scattering Experiments at Fermilab

J.G. Morfin[a]

[a]Fermilab, Batavia, IL USA

The future of deeply inelastic scattering experiments at Fermilab will be represented by neutrino experiments at the $\mathsf{MINOS}_{\mathsf{near}}$ detector site in the NuMI beam and, possibly in post-LHC timeframes, by high intensity neutrino beams from a muon collider/storage-ring source.

1. INTRODUCTION

Deep Inelastic Scattering (DIS) has a long and fruitful history at Fermilab through experiments involving both muons and neutrinos. The techniques involved range from the precise but low statistics bubble chamber experiments through massive electronic detectors with, comparatively, limited resolution. Although the cross section for neutrino scattering is many orders of magnitude smaller than the charged lepton cross section at HERA, the neutrino brings a new dimension to DIS since it has the ability to resolve the flavor of the quarks with which it interacts. The neutrino interacts with the $d, s, \bar{u}$ and $\bar{c}$ quarks while the antineutrino interacts with $u, c, \bar{d}, \bar{s}$. The neutrino is thus an ideal partner in investigating the partonic structure of the nucleon via the measurement of the structure functions.

The most recent DIS experiments at Fermilab have been performed in the neutrino area by the CCFR collaboration in its latest manifestation – NuTeV. Their latest results [1] represent the state-of-the-art for neutrino measurements of structure functions and are shown in Fig. 1 and Fig. 2. Fig. 1 displays the values $F_2(x, Q^2)$ vs Q^2 for given bands of x. The statistical errors of the data points range from (1–3)% with systematics about the same size. A similar plot for $xF_3(x, Q^2)$ is shown in Fig. 2. Here the statistical errors are somewhat larger ranging from (2–10)% with, again, systematic errors about the same size.

Although these latest results of CCFR are impressive, the experimenters still had to make two major compromises in their experimental technique. They had to use heavy nuclear targets

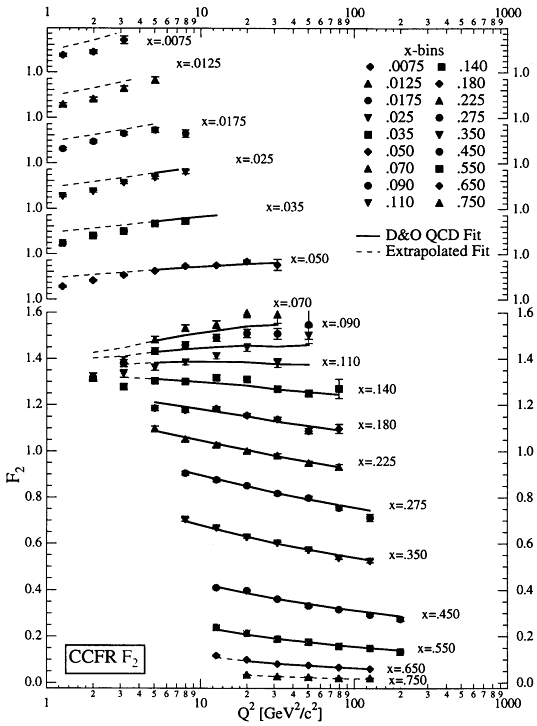

Figure 1. $F_2(x, Q^2)$ vs Q^2 for various x_{Bj} bands.

to accumulate sufficient statistics and, even having made this compromise, the statistics were not sufficient nor were the systematics sufficiently minimized to extract all possible information; namely independent ν and $\bar{\nu}$ values of F_2, xF_3 and $R = 2xF_1/F_2 - 1$. The six structure functions are shown in the following equations,

$$\frac{\mathrm{d}\sigma^{\nu N}}{\mathrm{d}x\mathrm{d}y} = \frac{G_F^2 ME}{\pi(1+Q^2/M_W^2)^2}\times$$

$$\Big[F_2^{\nu N}(x,Q^2)\left(\frac{y^2+(2Mxy/Q)^2}{2+2R_L^{\nu N}(x,Q^2)}+1-y-\frac{Mxy}{2E_{\bar{\nu}}}\right)$$

$$+xF_3^{\nu N}(x,Q^2)y\left(1-\frac{y}{2}\right)\Big] \quad (1)$$

$$\frac{\mathrm{d}\sigma^{\bar{\nu} N}}{\mathrm{d}x\mathrm{d}y} = \frac{G_F^2 ME}{\pi(1+Q^2/M_W^2)^2}\times$$

$$\Big[F_2^{\bar{\nu} N}(x,Q^2)\left(\frac{y^2+(2Mxy/Q)^2}{2+2R_L^{\bar{\nu} N}(x,Q^2)}+1-y-\frac{Mxy}{2E_{\bar{\nu}}}\right)$$

$$-xF_3^{\bar{\nu} N}(x,Q^2)y\left(1-\frac{y}{2}\right)\Big] \quad (2)$$

$$R_L(x,Q^2) = \frac{F_2(x,Q^2)}{2xF_1(x,Q^2)}(1-(2Mx/Q)^2)-1 \quad (3)$$

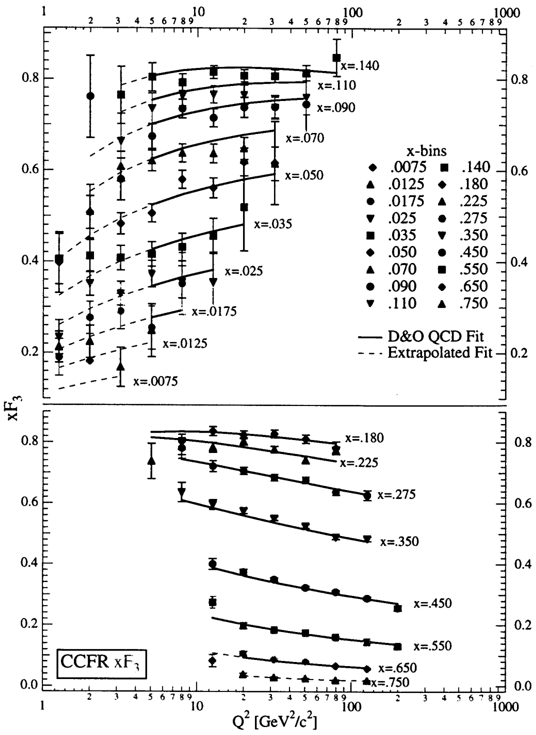

Figure 2. $xF_3(x,Q^2)$ vs Q^2 for various x_{Bj} bands.

2. MEASURING ALL SIX STRUCTURE FUNCTIONS

The method for extracting separate ν and $\bar{\nu}$ structure functions can be illustrated by expressing Eqs. (1) and (2) in the helicity representation and, initially, setting $R = 0$.

$$\frac{\mathrm{d}\sigma^{\nu A}}{\mathrm{d}x\mathrm{d}Q^2} = \frac{G_F^2}{2\pi x}\Big[\frac{1}{2}\left(F_2^{\nu A}(x,Q^2)+xF_3^{\nu A}(x,Q^2)\right)$$

$$+\frac{(1-y)^2}{2}\left(F_2^{\nu A}(x,Q^2)-xF_3^{\nu A}(x,Q^2)\right)\Big] \quad (4)$$

$$\frac{\mathrm{d}\sigma^{\bar{\nu} A}}{\mathrm{d}x\mathrm{d}Q^2} = \frac{G_F^2}{2\pi x}\Big[\frac{1}{2}\left(F_2^{\bar{\nu} A}(x,Q^2)-xF_3^{\bar{\nu} A}(x,Q^2)\right)$$

$$+\frac{(1-y)^2}{2}\left(F_2^{\bar{\nu} A}(x,Q^2)+xF_3^{\bar{\nu} A}(x,Q^2)\right)\Big] \quad (5)$$

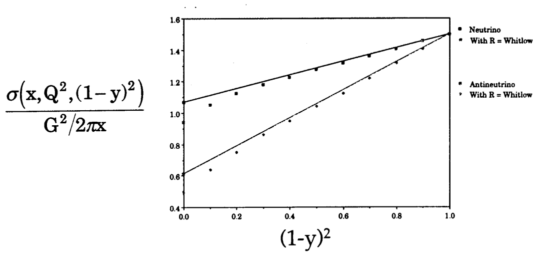

Figure 3. Weighted ν and $\bar{\nu}$ cross section vs $(1-y)^2$ for $x_{Bj} = 0.10$ and $Q^2 = 3$ GeV^2 for $R = 0$ (straight lines) and with $R = R$(Whitlow) (points).

As can be seen, when plotting $(1-y)^2$ vs $\sigma(x, Q^2, (1-y)^2)/(G_F^2/2\pi x)$, the equations represent a straight line with intercept $F_2 + xF_3$ and slope $F_2 - xF_3$ for ν and vice versa for $\bar{\nu}$ With $R \neq 0$, a y^2 term is introduced and the straight line becomes a curve as shown in Fig. 3 . For this figure, CTEQ5M pdfs were used and R was taken from [2].

There are considerable challenges in extracting all six structure functions in this manner. Enormous statistics are needed not only to populate the $x - Q^2$ plane but to enable sufficient $(1-y)^2$ bins within each $x - Q^2$ space to fit R, the slope and the intercept. Beam systematics must be controlled to minimize the "wiggle" in the fitted slope and intercept. Systematics in the measured kinematical quantities must also be minimized to control migration and smearing in this 3-dimensional space.

Are the rewards worth the effort? Recall that ν and $\bar{\nu}$ are able to resolve the flavors of the quarks with which they interact. In the parton model, F_2 and xF_3 can be expressed as follows,

$$F_2^{\nu N}(x, Q^2) = x[u + \bar{u} + d + \bar{d} + 2s + 2\bar{c}] \quad (6)$$
$$F_2^{\bar{\nu} N}(x, Q^2) = x[u + \bar{u} + d + \bar{d} + 2\bar{s} + 2c] \quad (7)$$
$$xF_3^{\nu N}(x, Q^2) = x[u + d - \bar{u} - \bar{d} + 2s - 2\bar{c}] \quad (8)$$
$$xF_3^{\bar{\nu} N}(x, Q^2) = x[u + d - \bar{u} - \bar{d} - 2\bar{s} + 2c] \quad (9)$$

It is easy to see that:

$$F_2^{\nu} - F_2^{\bar{\nu}} = s - \bar{s} + c - \bar{c} \qquad (10)$$

while $xF_3^{\nu} - xF_3^{\bar{\nu}} = s + \bar{s} - c + \bar{c}$ yields an independent measure of the strange sea to check the other neutrino measurement using di-lepton production in $\bar{\nu}$. If we assume $s = \bar{s}$ and $c = \bar{c}$ we can combine the last expression with:

$$F_2^{\nu} - xF_3^{\nu} = 2(\bar{u} + \bar{d} + 2\bar{c}) \qquad (11)$$

and

$$F_2^{\bar{\nu}} - xF_3^{\bar{\nu}} = 2(\bar{u} + \bar{d} + 2\bar{s}) \qquad (12)$$

to extract $\bar{u} + \bar{d}$, c and s in each $x - Q^2$ bin.

3. NUCLEAR EFFECTS IN NEUTRINO INTERACTIONS

From experiments with charged leptons off various nuclear targets, we know that the ratio of F_2/nucleon between two different nuclei behaves as in Fig. 4. As we increase x_{Bj} from 0 we pass through regions dominated by "shadowing", "anti-shadowing", "EMC effect" and, for $x_{Bj} \geq 0.7$, the "Fermi motion" effects.

Note that all of this data is for muon or electron scattering. There is no high statistics data for neutrino-nucleus interactions so we have no accurate measurements of nuclear effects with ν and $\bar{\nu}$ beams. This has led to a serious problem in comparing neutrino scattering results with muon scattering results in the "shadowing" regions $x < 0.1$.

After correcting the NMC [3] measurements of F_2 for nuclear effects of Fe we still find a significant difference when comparing these with the CCFR [1] measurements of ν-Fe corrected for the difference in coupling strengths between muon and neutrino interactions:

$$F_2^{\mu} = \frac{5}{18} F_2^{\nu} - \frac{1}{6} x(s + \bar{s}) \qquad (13)$$

Fig. 5 shows F_2 vs Q^2 at three values of x. The CCFR values of F_2 are systematically higher than those of NMC. As x increases, the difference becomes progressively smaller and disappears at $x \approx 0.1$, placing the disagreement squarely in the "shadowing" region.

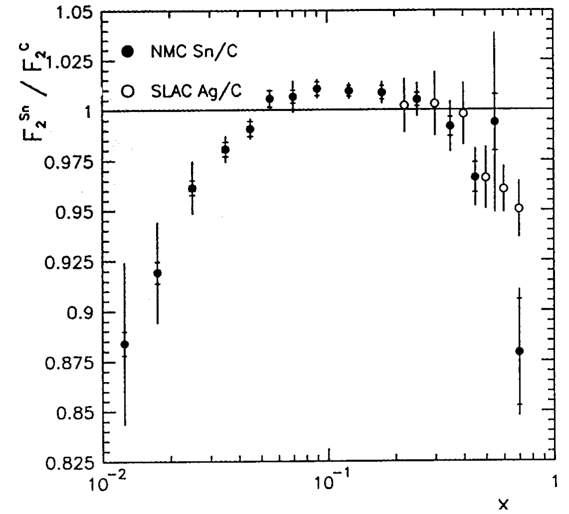

Figure 4. F_2 per nucleon on Sn divided by F_2 on C vs x_{Bj} as measured by the NMC collaboration.

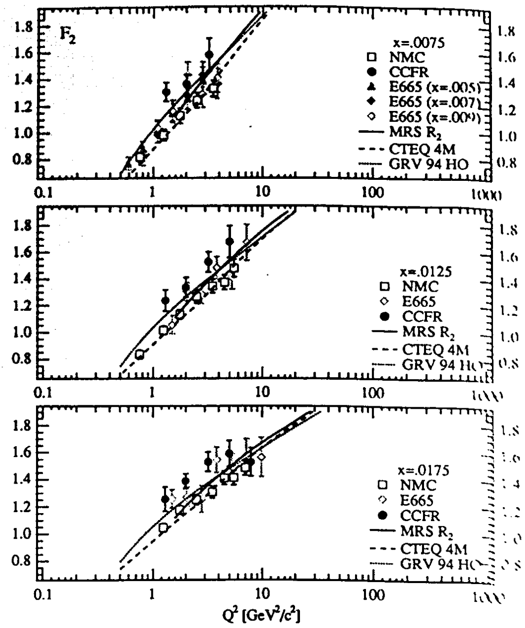

Figure 5. F_2 vs Q^2 as measured by the CCFR and NMC collaborations for three x_{Bj} bands.

Both the NMC and CCFR collaborations have checked and rechecked their results and have found no explanation for this difference. A recent paper by C. Boros et al. [4] has attributed this difference to a charge symmetry violation in the sea quarks. They predict $\nu - A$ to $\nu - N$ shadowing corrections based on CVC and the addition of axial vector meson modes to traditional vector meson dominance explanation for shadowing. The c.s.v term they extract from the difference is quite large, comparable in magnitude to the s-quark distribution function in this region of x.

Among other, less dramatic, explanations of this difference is that we simply do not understand shadowing in $\nu - A$ interactions. Can we measure these nuclear effects with neutrinos at Fermilab?

4. NEAR-FUTURE DEEPLY INELASTIC SCATTERING EXPERIMENTS AT FERMILAB

The near future at Fermilab will be enriched by the new accelerator designed to replace the nearly 30 year old Main Ring. The Fermilab Main Injector (MI) has been officially commissioned and is already providing increased protons to the Tevatron for the on-going (final) 800 GeV Fixed Target run. The MI will provide a highly intense beam of 120 GeV protons to the Neutrinos at the Main Injector (NuMI) program starting in late 2002. The neutrino beam will consist of a long (2 λ) target and two focusing parabolic horns. The target and second horn can be moved with respect to the first horn to give three different beam configurations: low-energy (le), medium-energy (me) and high-energy (he) with event rates at the $\mathsf{MINOS_{near}}$ detector shown in Fig. 6. Since the primary goal of NuMI is the detection and study of neutrino oscillations with the $\mathsf{MINOS_{near}}$ and far detectors, knowledge of the spectra of neutrinos must be excellent. A separate fixed target experiment in the Fermilab Meson area will measure the spectra of π, K and p produced when 120 GeV protons are directed to the NuMI target. The goal is to know the absolute flux and energy dependent spectra to better than 2%.

In the high-energy configuration, with a nominal 3.7×10^{20} protons on the NuMI target per year, the NuMI beam will yield 2.5 million neutrino events per year per ton of detector at the $\mathsf{MINOS_{near}}$ detector located 1 km from the target. $\bar{\nu}$ production will be down by a factor of 4. The $\mathsf{MINOS_{near}}$ detector will be 17 m long magnetized iron/scintillator spectrometer divided into four sections. In the first three sections (veto, target, hadron shower), solid scintillator planes with fiber readout will alternate with 2.5 cm thick iron plates. In the last 9.5 m muon spectrometer section only every fifth gap will have solid scintillator. The solid scintillator will cover out to $r \approx 1$ m from beam center. Choosing a fiducial volume of $r = 80$ cm means a fiducial mass for each plate of 0.4 ton which, in turn, implies an event rate of 1 million events per plate per year. With 40 planes in the target section, the $\mathsf{MINOS_{near}}$ detec-

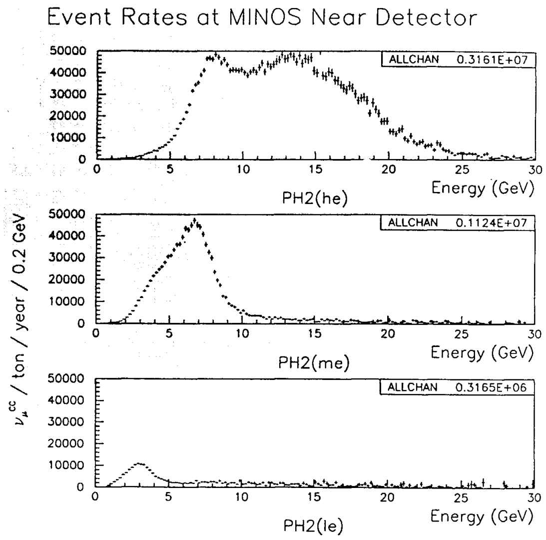

Figure 6. The energy distribution of neutrino CC event at the $\mathsf{MINOS_{near}}$ detector for the high energy, medium energy and low energy configurations.

tor will accumulate 40 million neutrino events per year. This 1-year total is probably close to being more than the sum of all other experiment's neutrino fiducial events from the beginning of accelerator neutrino experiments. With a W^2 (mass of the hadron system) cut of 5 GeV^2 to select DIS there are still more than 25 million events with Q^2 ranging up to 25 GeV^2 and $.01 < x < .95$.

4.1. Extracting ν and $\bar{\nu}$ Structure Functions with MINOS

As an example of the accuracy obtainable with the $\mathsf{MINOS_{near}}$ detector, in the $x - Q^2$ bin corresponding to the expected $(1-y)^2$ behavior shown in Fig. 3 ($.10 < x < 0.12$ and $2 < Q^2 < 4$) the expected rate in this single bin is 650.000 events per year ν and just under 100.000 $\bar{\nu}$ events. Assuming 2 years of neutrino and 2 years of antineutrino running, the errors on the measured points in the σ vs $(1-y)^2$ plane for ν and $\bar{\nu}$ will be completely dominated by the systematic error (estimated $< 2.5\%$) except for the kinematicaly limited low y region which translates to high $(1-y)^2$. The author is presently increasing Monte Carlo statistics and testing a fitting program to determine the consequent errors on the extracted structure functions themselves.

4.2. Measuring Nuclear Effects in ν-nucleus Interactions

The measurement of nuclear effects will require a modification of the $\mathsf{MINOS_{near}}$ detector. Plates of different A values must be added to the detector. There is sufficient room to add these to the detector without modifying the present support structure. To illustrate the potential of such a modified MINOS detector, consider the addition of six (instrumented) planes of C (graphite), 4 "bags" of Be and one plane of tungsten which needs to be only 1.75 cm thick instead of 2.5 cm to match the sum carbon statistics of 2 million events per year. The different A-targets will be exposed simultaneously so beam systematics cancel when taking ratios of F_2 off each of the targets. The Be - C - Fe - W relative target systematics is taken as $O(1\%)$ as in experiments using charged leptons on various A targets. Fig. 7 shows the expected errors on the ratios of F_2/nucleon from a 2-year run. There are no errors shown on the W/Be ratio since the plastic wrap on the Be presents an unknown systematic. For the bin at $x = 0.01$ we are simply running out of statistics. However, at $x = 0.02$ with the ratio of W/C, there would be a 5 s.d. shadowing signal if shadowing with neutrinos was at least as strong as shadowing with muons.

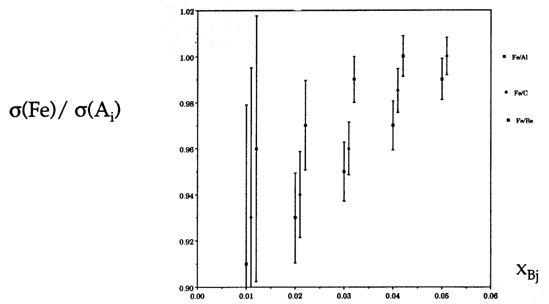

Figure 7. The ratio of F_2 for various A-values as a function of x_{Bj}.

5. FURTHER IN THE FUTURE: NEUTRINOS FROM A MUON STORAGE-RING/COLLIDER

Both Europe and the US are dedicating considerable research time into the possibility of constructing a muon-collider as the next (post-LHC) high energy research facility. The physics possible with colliding muons is quite impressive and has been summarized in several publications. As the machine designers were considering radiation hazards associated with the high-intensity rings they noticed that one of the hazards was the huge flux of neutrinos, coming from the decaying muons, which could interact in the vicinity of people producing large hadronic showers which were the actual radiation hazard. It did not take long before this possible radiation hazard became a possible source of high intensity neutrinos [6] for both neutrino oscillation and DIS experiments.

5.1. Steps to Produce Neutrinos from a Muon Storage Ring

The proton source for a muon collider must be intense producing 10^{21-22} 8-16 GeV protons per year. The new Fermilab MI will eventually produce around 10^{21} 120 GeV protons per year for comparison. The target for the muon collider source is still under study. The thought is that since such intensities would probably liquify any solid target why not start out with a liquid target to begin with. The low energy pions which are produced are captured by a massive solenoid field and directed into a decay channel. The resulting muons are then "cooled" via ionization cooling to minimize the multi-dimensional phase-space and to form a "bunch" which can then be accelerated. A recirculating LINAC accelerates the muons to a desired energy and the muons, as a source of neutrinos, are injected into a storage ring with long straight sections.

5.2. Characteristics of the Neutrino Beam

With a 250 GeV muon storage ring a DIS experiment with detector consisting of a 1 m long Hydrogen target located a km away from the straight section would record 18 million ν_μ and 10 million $\bar{\nu}$ per year. The neutrino flux would be known to 0.1% and would have a shape as in Fig. 8. The spectrum on the left comes from the 250 GeV ring itself while the spectrum on the right results from muon decays while in the recirculating linac.

This would be the ultimate neutrino deep inelastic experiment yielding high statistics while using a nucleon target with negligible beam and detector systematics.

Acknowledgements: I would like to thank J.I. Illana and A. Hagedorn for technical assistance during the write-up of this paper.

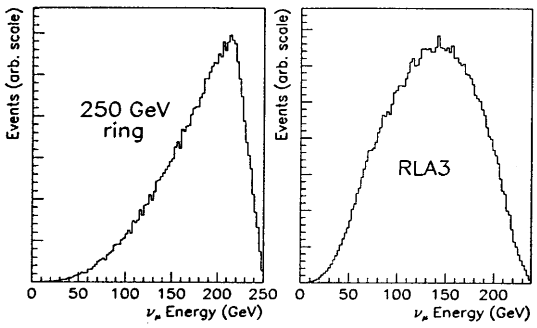

Figure 8. The energy distribution of neutrino CC event resulting from muon decay in (left) a 250 GeV muon storage ring and (right) the recirculating LINAC.

REFERENCES

1. U.K. Yang, these proceedings.
2. L.W. Whitlow et al., Phys. Lett **B250** (1990) 193.
3. P. Amaudruz et al., Z. Phys. C51 (1991) **387**, and references therein.
4. C. Boros et al., hep-ph/9810220.
5. H.L. Lai et al., submitted to Eur. Phys. J. **C**, May 1999.
6. S. Geer, Phys. Rev. **D57** (1998) 1.